JACS
JOURNAL OF THE AMERICAN CHEMICAL SOCIETY
Article
pubs.acs.org/JACS

Water–Polysaccharide Interactions in the Primary Cell Wall of *Arabidopsis thaliana* from Polarization Transfer Solid-State NMR

Paul B. White,[†,§] Tuo Wang,[†,§] Yong Bum Park,[‡] Daniel J. Cosgrove,[‡] and Mei Hong*[,†]

[†]Department of Chemistry and Ames Laboratory, Iowa State University, Ames, Iowa 50011, United States
[‡]Department of Biology, Pennsylvania State University, University Park, Pennsylvania 16802, United States

Supporting Information

ABSTRACT: Polysaccharide-rich plant cell walls are hydrated under functional conditions, but the molecular interactions between water and polysaccharides in the wall have not been investigated. In this work, we employ polarization transfer solid-state NMR techniques to study the hydration of primary-wall polysaccharides of the model plant, *Arabidopsis thaliana*. By transferring water ^{1}H polarization to polysaccharides through distance- and mobility-dependent ^{1}H–^{1}H dipolar couplings and detecting it through polysaccharide ^{13}C signals, we obtain information about water proximity to cellulose, hemicellulose, and pectins as well as water mobility. Both intact and partially extracted cell wall samples are studied. Our results show that water–pectin polarization transfer is much faster than water–cellulose polarization transfer in all samples, but the extent of extraction has a profound impact on the water–polysaccharide spin diffusion. Removal of calcium ions and the consequent extraction of homogalacturonan (HG) significantly slowed down spin diffusion, while further extraction of matrix polysaccharides restored the spin diffusion rate. These trends are observed in cell walls with similar water content, thus they reflect inherent differences in the mobility and spatial distribution of water. Combined with quantitative analysis of the polysaccharide contents, our results indicate that calcium ions and HG gelation increase the amount of bound water, which facilitates spin diffusion, while calcium removal disrupts the gel and gives rise to highly dynamic water, which slows down spin diffusion. The recovery of spin diffusion rates after more extensive extraction is attributed to increased water-exposed surface areas of the polysaccharides. Water–pectin spin diffusion precedes water–cellulose spin diffusion, lending support to the single-network model of plant primary walls in which a substantial fraction of the cellulose surface is surrounded by pectins.

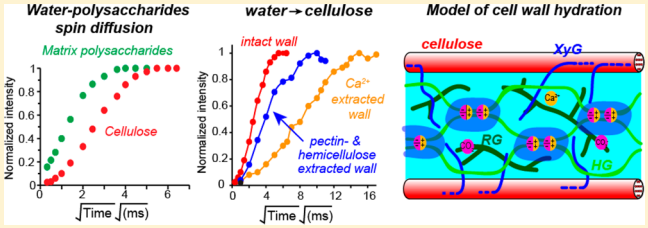

INTRODUCTION

The primary cell wall of growing plants contains a mixture of polysaccharides and glycoproteins that provide mechanical strength to the cell, protect cells against biotic and environmental stresses, and allow cell–cell adhesion.[1,2] At the core of this polysaccharide mixture are nanometer-sized cellulose microfibrils, which interact with matrix polysaccharides. In dicotyledonous plants such as *Arabidopsis thaliana*, these matrix polysaccharides mainly consist of the neutral hemicellulose, xyloglucan (XyG), and negatively charged pectins, which are galacturonic acid (GalA)-rich polymers. Two major types of pectins are found in dicot primary walls: the linear homogalacturonan (HG) and rhamnogalacturonan I (RGI), which contains arabinan (Ara) and galactan (Gal) side chains of varying lengths.

The molecular packing and three-dimensional architecture of primary wall polysaccharides have been extensively characterized by chemical extraction and biochemical assays. Recent evidence from 2D and 3D solid-state NMR spectroscopy[3−6] and biomechanical studies of endoglucanase-treated cell walls[7] suggests that, in contrast to the conventional tethered network model,[8] cellulose microfibrils are in close contact with both pectins and hemicellulose on the sub-nanometer scale, but the microfibrils are neither mechanically tethered by XyG nor extensively coated with XyG. This polysaccharide network exhibits heterogeneous mobility: the cellulose chains are immobilized by intra- and intermolecular hydrogen bonding and hydrophobic interactions, whereas pectins exhibit large-amplitude motion. This motional heterogeneity is manifested by the selective detection of pectin signals in certain solid-state NMR spectra[3,4,9,10] and by different nuclear-spin relaxation times.[11−13] The mobility of hemicellulose is intermediate between those of cellulose and pectins.[4]

A different approach for investigating the structure and dynamics of the plant cell wall is to probe the water accessibilities of polysaccharides. Water is a prerequisite for wall-degrading enzymes and is essential for polymer creep of the primary wall during growth. Cell wall hydration depends on the ionic content and intermolecular packing of the polysaccharides. It is well-known that anionic pectins strongly attract water and are the main swelling agent of the cell wall.[14] Indirect evidence of preferential hydration of pectins in the wall is seen in the reduced pectin intensities in ^{13}C cross-

Received: April 24, 2014
Published: July 1, 2014

dx.doi.org/10.1021/ja504108h | J. Am. Chem. Soc. 2014, 136, 10399–10409

Table 1. Relative Intensities of Polysaccharide ^{13}C Signals of *Arabidopsis* Primary Walls from Quantitative 1D ^{13}C Spectra[a]

^{13}C chemical shift (ppm)	assignment	sample 1	assignment changes	sample 2	sample 3	sample 4
108	A C1	1.00		0.90	0.84	0.58
101	R/HG C1	1.00		0.49	0.38	0.35
100	GA/x C1	1.00	(H)GA/x C1	1.36	0.75	0.44
99	GA/x C1	1.00		0.78	0.65	0.48
80	(H)GA C4, R C2	1.00		0.48	0.40	0.37
78	Gal C4, A C3	1.00	(H)GA C4, R C2, Gal C4, A C3	1.25	0.79	0.53
69	(H)GA C2, R C5	1.00		0.84	0.55	0.34
53	methyl ester	1.00		0.24	0.15	0.17
21	acetyl	1.00		0.57	0.21	0.19
17	R C6	1.00		0.79	0.51	0.32
105	i/s/G/Gal C1	1.00		1.02	0.90	0.89
89	i C4	1.00		1.00	1.00	1.00
65	i C6	1.00		0.99	0.89	0.96
62	i/s/Gal/G C6, x/A C5	1.00		1.02	0.83	0.79

[a]The intensities are normalized to the height of the 89 ppm cellulose C4 peak in each sample, and then normalized to the value of sample 1.

polarization (CP) NMR spectra of hydrated cell walls compared to dry walls,[10] because hydration-induced pectin motion reduces the $^1H-^{13}C$ dipolar coupling that drives CP. But direct measurement of pectin–water interaction has not been reported. Cellulose–water and hemicellulose–water interactions in native cell walls are even less studied. Molecular mechanics simulations of cellulose–water interactions found that water changes the hydroxymethyl (C6) conformation of the glucan chains to increase interlayer hydrogen bonds[15] and may cause twisting of cellulose Iβ fibrils under certain conditions. These simulations also showed that water can be well ordered on cellulose surfaces by a combination of hydrogen-bonding and hydrophobic hydration of nonpolar surfaces. But experimental data of cellulose–water interactions in native plant cell walls are scarce.[16]

In this study, we investigate the water–polysaccharide interaction in the primary walls of *Arabidopsis thaliana* using solid-state NMR techniques that transfer the water ^1H polarization to polysaccharides. While several mechanisms of polarization transfer exist, our experimental conditions emphasize the mechanisms of chemical exchange followed by spin diffusion, which is mediated by distance- and mobility-dependent $^1H-^1H$ dipolar couplings. By detecting the water-transferred polysaccharide ^{13}C signals as a function of mixing time, we obtain information about the water proximities of the polysaccharides as well as the water dynamics in the wall. This ^1H spin diffusion approach has been extensively used to study proteins in crystalline[17] and membrane environments.[18−21] For plant cell walls, spin diffusion NMR has been used to determine the carbohydrate-binding target of a wall-loosening protein, expansin.[22] We examine four *Arabidopsis* primary wall samples, in which pectins and XyG were sequentially extracted by chelating agents, weak base, and endoglucanases. We show that the mobility and distribution of water in these samples differ significantly even though the total water contents are similar. The polarization transfer rates are strongly affected by the concentration and extent of HG esterification and by the relative amounts of matrix polysaccharides to cellulose. These results reveal a profound effect of HG on water mobility and the impact of extraction on the water-exposed surface areas of polysaccharides in the wall.

EXPERIMENTAL SECTION

Plant Material. Uniformly ^{13}C-labeled *Arabidopsis thaliana* primary walls were prepared from seedlings grown in liquid culture[4,22] using a procedure adapted from Gibeaut and co-workers.[23] The walls were never dried throughout the preparation. Plant tissue was frozen at −80 °C, ground in liquid nitrogen, and incubated with shaking in 1.5% sodium dodecyl sulfate (SDS) at room temperature (RT) for 3 h to inactivate endogenous wall-degrading enzymes. The tissue was washed 10 times with double-distilled water (ddH_2O), incubated with shaking at 37 °C for 12 h in 50 mM MES buffer (pH 6.8) that contains porcine pancreas α-amylase (5000 units, 30 mL^{-1}) to remove starch and 0.02% NaN_3 to inhibit microbial growth. The walls were washed again three times with ddH_2O, incubated with shaking at 40 °C for 12 h in 50 mM MES buffer (pH 7.5) that contains Pronase (200 units, 5 mg 20 mL^{-1}) to further digest proteins and 0.02% NaN_3 to inhibit microbial growth. The sample was washed again three times with ddH_2O, incubated with shaking in 1.5% SDS at RT for 1 h to inactivate Pronase, and washed 10 times with 0.02% NaN_3 as a final step to prevent microbial contamination during storage and NMR experiments.

The intact cell walls prepared above were subjected to sequential extraction to create a total of four NMR samples. Sample 1 is the unextracted wall, while the other three samples were sequentially treated with *trans*-1,2-cyclohexanediaminetetraacetic acid (CDTA), sodium carbonate (Na_2CO_3), xyloglucanase (XEG), and Cel12A to selectively remove matrix polysaccharides. Sample 2 was extracted with 50 mM CDTA (pH 6.5) overnight (with three exchanges), followed by a second overnight extraction with three exchanges of 50 mM Na_2CO_3 containing 20 mM $NaBH_4$. CDTA chelates calcium ions (Ca^{2+}), which removes the ionic cross-links between the carboxyl groups of HG, thus solubilizing HG. Na_2CO_3 neutralizes GalA and hydrolyzes methyl esters to carboxylate ions, further solubilizing HG. Na_2CO_3 also hydrolyzes the esters in RGI. However, most GalA in RGI is not methyl-esterified but is acetylated at O3, and acetyl groups are more resistant to hydrolysis because of the bulkiness of the sugar, the electronic effects of the secondary alcohol, and the presence of neutral side chains in RGI, which make RGI more hemicellulose-like than HG.

Sample 3 was sequentially treated with CDTA, Na_2CO_3, and XEG (200 μg mL^{-1}), a recombinant XyG-specific endoglucanase.[24,25] The treatment with XEG was carried out in 100 mM ammonium acetate (pH 5.0) with 0.02% NaN_3 at 37 °C for 48 h to remove the majority of non-load-bearing XyG[7] Sample 4 was sequentially treated with CDTA, Na_2CO_3, XEG, and an evolved Cel12A (200 μg mL^{-1}). Cel12A is a recombinant endoglucanase that digests some of the load-bearing XyG and noncrystalline cellulose.[7] We used a variant of Cel12A evolved for higher expression in *Escherichia coli*.[26] The extraction with Cel12A was carried out in 100 mM ammonium acetate (pH 4.0) containing 0.02%

Table 2. (Top) Monosaccharide Compositions (Mol % of Total Sugars, ±SEM, n = 3 Technical Replicates) of the Four Cell Wall Samples Used for NMR Analysis and (Bottom) Cell Wall Compositions (%) Estimated from the Sugar Analysis

Monosaccharide Composition of the Cell Wall Samples Used for NMR Analysis[a]								
sample	Fuc	Rha	Ara	Gal	Glc[b]	Xyl/Man[b]	GalA	GluA
1	1.5 ± 0.03	10.0 ± 0.09	10.4 ± 0.18	9.5 ± 0.14	8.0 ± 0.13 (20.2 ± 0.75)	15.8 ± 0.37 (0.9 ± 0.02)	23.8 ± 0.38	0.3 ± 0.19
2	1.7 ± 0.06	9.9 ± 0.16	12.9 ± 0.21	10.8 ± 0.13	10.7 ± 0.18 (22.9 ± 0.29)	17.9 ± 0.09 (1.6 ± 0.14)	11.6 ± 0.10	0.1 ± 0.05
3	1.5 ± 0.05	10.3 ± 0.05	13.6 ± 0.19	10.5 ± 0.11	5.8 ± 0.10 (26.2 ± 0.53)	18.1 ± 0.42 (2.1 ± 0.27)	11.7 ± 0.28	0.2 ± 0.07
4	1.4 ± 0.03	9.9 ± 0.15	13.1 ± 0.12	10.1 ± 0.03	5.5 ± 0.07 (29.1 ± 0.67)	17.5 ± 0.6 (1.9 ± 0.20)	11.4 ± 0.27	0.1 ± 0.07

Cell Wall Composition from Sugar Analysis[c]				
sample	cellulose	xyloglucan	xylan/mannan	pectin
1	20.2 ± 0.7	16.0 ± 0.3	11.9 ± 0.5	51.8 ± 0.4
2	22.9 ± 0.3	21.5 ± 0.4	12.7 ± 0.2	42.9 ± 0.4
3	26.2 ± 0.5	11.6 ± 0.2	17.5 ± 0.1	44.7 ± 0.3
4	29.1 ± 0.7	11.0 ± 0.1	16.9 ± 0.2	42.9 ± 0.5

[a]Method used 2 M TFA (H_2SO_4 hydrolysis of residue). [b]The top number in each entry shows the sugars, primarily from matrix polysaccharides, released by methanolysis and hydrolysis of the samples with 2 M trifluoracetic acid (TFA). The bottom number, in parentheses, shows sugars in the residues (mainly cellulose). Our analysis did not separate xylose from mannose. [c] Using a method described by Wang et al. in 2013.[22]

NaN_3 at 37 °C for 48 h. Avicel PH-101 was purchased from Sigma-Aldrich and used as received.

The cell wall samples were centrifuged at 1000g for 5 min and 5000g for 90 min to reach a hydration level of ∼40 wt%, as verified by gravimetric analysis of the unextracted wall. Monosaccharide compositions of the four samples were analyzed as described previously,[22] but with the addition of a methanolysis step[27] before hydrolysis with trifluoracetic acid, which otherwise reduces galacturonic acid content by up to 70%.

About 65 mg of each cell wall sample was packed into 4 mm magic-angle-spinning (MAS) rotors for solid-state NMR experiments. Intensity quantification (Table 1) and sugar composition analysis (Table 2) were used to estimate the relative concentrations of pectins, XyG and cellulose in the four samples.

Solid-State NMR Experiments. Experiments were conducted on a Bruker Avance II 600 MHz spectrometer (14.1 T) using a 4 mm MAS probe. Typical radiofrequency (rf) field strengths were 66−71 kHz for ^{1}H decoupling and 50 kHz for ^{13}C pulses. Most experiments were conducted under 9 kHz MAS. ^{13}C chemical shifts were externally referenced to the adamantane CH_2 signal at 38.38 ppm on the TMS scale.[28]

The pulse sequence for the water−polysaccharide polarization transfer experiment is shown in Figure 1a.[19,21,29−31] In the 1D experiment, a ^{1}H T_2 filter of 1.2−2.6 ms was used to suppress the polysaccharide magnetization while retaining most water magnetization. More than 97% of the polysaccharide ^{13}C signals were removed by the ^{1}H T_2 filter while the water ^{1}H signal remained at 60−80% (Figure 1b,c). After the T_2 filter, the water ^{1}H polarization was transferred to polysaccharide protons during a mixing time (t_{m1}). Three mechanisms can be present to mediate polarization transfer: chemical exchange, nuclear Overhauser effect (NOE), and spin diffusion. Chemical exchange requires labile protons, which are present as OH groups in all polysaccharides; thus this mechanism is uniformly active for all samples. NOE is a dipolar cross relaxation phenomenon that manifests most clearly under ultrafast MAS.[32,33] At the moderate MAS frequency of 9 kHz used here, NOE is expected to be insignificant. Spin diffusion is mediated by coherent ^{1}H−^{1}H dipolar coupling, which depends on both internuclear distances and mobility, and is important at moderate MAS frequencies. Thus, in our experiments the main mechanism of water−polysaccharide polarization transfer is chemical exchange followed by spin diffusion, and the buildup curves reflect water−polysaccharide distances as well as the dynamics of water and polysaccharides.

After the mixing period, 500 μs of Hartman−Hahn cross-polarization (HH-CP) transfers the polysaccharide ^{1}H magnetization to ^{13}C for detection. Monitoring the ^{13}C intensities as a function of t_{m1} gives site-specific polarization transfer buildup curves. Since spin diffusion is active during the HH-CP period at half the rate as the longitudinal spin diffusion rate, there is a 250 μs additional effective spin diffusion time, but this time contribution is negligible compared to the t_{m1} periods.

To better resolve the signals of water-accessible polysaccharides, we extended the 1D experiment to 2D by adding a ^{13}C chemical shift evolution period (t_1) and a mixing period (t_{m2}) after the CP step. The t_{m2} period was short, 10 ms, to restrict cross peaks to intramolecular correlations. When the ^{1}H T_2 filter is removed, we obtain 2D spectra showing all polysaccharide signals irrespective of water exposure. The 1D and 2D ^{1}H spin diffusion experiments were conducted at 263 K where pectins and hemicellulose are significantly immobilized.

Quantitative 1D ^{13}C spectra were measured at 293 K using ^{13}C direct polarization (DP) and a recycle delay of 25−30 s, which is sufficient for complete relaxation of these uniformly ^{13}C-labeled cell wall samples, whose longest ^{13}C spin−lattice relaxation times are ∼6.7 s. 1D ^{1}H DP spectra were measured at 296 K with a recycle delay of 10 s to quantify the water content of the samples. 2D ^{13}C J-INADEQUATE spectra[34−36] were measured at 296 K using ^{13}C DP and a short recycle delay of 2 s to preferentially detect the signals of matrix polysaccharides. 2D ^{13}C spin diffusion correlation (DARR) spectra[37] with 30 ms mixing were measured at 253 K to verify the polysaccharide concentrations. A dipolar-doubled C−H DIPSHIFT experiment[38] was conducted to measure polysaccharide mobility. The FSLG sequence[39] was used for ^{1}H homonuclear decoupling. The scaling factor was verified to be 0.577 based on measurements of the rigid model peptide formyl-Met-Leu-Phe.[40,41] The measured coupling was converted to the true coupling using $\omega_{CH}^{true} = (\omega_{CH}^{meas}/(2 \times 0.577))$. The ratio of the true coupling to the rigid-limit value (22.7 kHz) gives the order parameter.

A ^{1}H-undecoupled 2D ^{1}H−^{13}C correlation experiment was conducted at 295 K to measure the ^{1}H chemical shift of polysaccharide-bound water. The experiment used a spin diffusion mixing time of 0.1 ms for sample 1 and 2 ms for sample 2.

RESULTS

Polysaccharide Compositions of Sequentially Extracted Cell Walls. Quantitative ^{13}C spectra were measured using recycle delays of 25−30 s to determine the polysaccharide contents and their changes due to sequential extraction. The intact wall shows well-resolved ^{13}C signals for matrix polysaccharides and crystalline cellulose (Figure 2a). Partic-

dx.doi.org/10.1021/ja504108h | J. Am. Chem. Soc. 2014, 136, 10399−10409

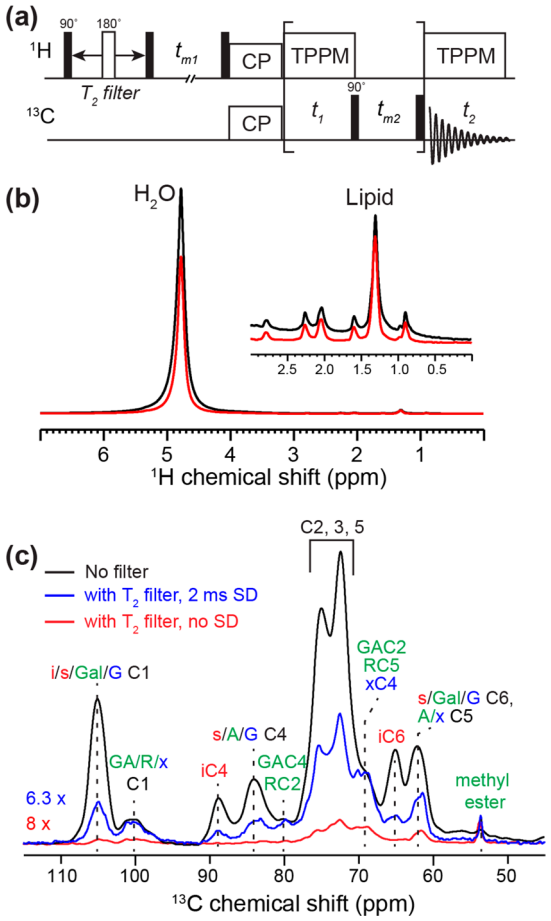

Figure 1. (a) Pulse sequence of the water–polysaccharide spin diffusion experiment. The 2D version is shown here. Removal of the t_1 and t_{m2} periods converts the experiment to 1D. (b) ^{1}H spectra of sample 1 without (black) and with (red) a T_2 filter (1.6 ms). Inset shows a 32-fold *y*-axis enlarged spectrum of the lipid ^{1}H chemical shift region. (c) ^{13}C CP-MAS spectra of sample 1 without T_2 filter (black), with a 1.6 ms ^{1}H T_2 filter but no spin diffusion (SD) (red), and with a 1.6 ms T_2 filter and 2 ms spin diffusion (blue). The ^{1}H and ^{13}C spectra were measured at 263 K under 9 kHz MAS. Assignment abbreviations:[4] i, interior crystalline cellulose; s, surface cellulose; G, glucose in xyloglucan; x, xylose; A, arabinan; R, rhamnose; GA and GalA, galacturonic acid; Gal, galactan.

ularly useful for assignment and quantification are the 89 ppm peak of crystalline cellulose C4, the 101 ppm peak of HG and rhamnose (Rha) C1,[4] the 99 ppm peak of GalA and xylose (Xyl) C1, the 80 ppm peak of GalA C4 and Rha C2, the 65 ppm peak of crystalline cellulose C6, and the 53 ppm peak of methyl ester in HG.

Extraction by CDTA and Na_2CO_3 nearly completely suppressed the 53 ppm methyl ester peak (Figure 2b), indicating hydrolysis of methyl esters to carboxylate and methanol. The 101 ppm peak is also suppressed, accompanied by a significant increase of the 100 ppm peak, suggesting that the HG C1 chemical shift changed to 100 ppm (Table 1). Thus, the 100 ppm peak in sample 2 should include not only RGI GalA and Xyl C1, but also C1 of the unextracted HG. The C4 chemical shift of GalA also changed from 79.5 to 78.6 ppm from sample 1 to sample 2.[4]

The carbonyl region of the spectrum exhibits structurally informative changes (Figure S1). The intact wall exhibits three resolved carbonyl peaks: the 172 ppm methyl ester peak, which mostly originates from HG; the 174 ppm acetyl peak, which largely results from RGI; and the 176 ppm carboxylate peak, which can result from both HG and RGI. The strong 172 ppm peak of GalA C6 is present in sample 1 but absent in sample 2, and is replaced by a 176 ppm carboxylate peak, confirming that methyl esters have been converted to carboxylates. Since both samples are near neutral pH, well above the GalA pK_a of ~3.5, the change of the 176 ppm peak intensity cannot be attributed to GalA protonation or deprotonation. The 174 ppm acetyl peak is little changed between samples 1 and 2, suggesting that RGI is relatively unaffected in sample 2. This is verified by the intensities of other peaks in the 1D quantitative ^{13}C spectra and 2D correlation spectra, all of which indicate that the RGI was retained to ~90% in sample 2 whereas HG concentration decreased to ~64% (Tables S1 and S2). Interestingly, although the total pectin concentration is lower in sample 2, the integrated COO^- signals in the quantitative spectra are similar between the two samples (Figure 2a,b), indicating that the loss of HG is offset by the conversion of methyl esters to carboxylates. The 176 ppm COO^- peak is also much narrower in sample 2, suggesting that the non-cross-linked HG chains have either larger mobility or more uniform conformation.

Additional digestion by XEG reduced the intensities of the 99 ppm peak, the 79 ppm peak, and the 68 ppm peak (Figure 2c), which correspond to GalA/Xyl C1, GalA C4 and Rha/Ara C2, and Rha/Ara C5 and GalA/HG C2, respectively. These changes indicate that XyG as well as RGI are extracted by XEG, which may occur to XyG-bound pectins during the washing step. Assuming that the cellulose concentration is constant in these samples, the total pectin concentration in sample 3 is about half the pectin concentration of the intact wall, whereas the XyG concentration in sample 3 is ~70% that of the intact wall (Tables S2 and S3). Finally, the Cel12A-extracted sample 4 shows only 30% and 40% of the pectin and hemicellulose quantities as the intact sample. For comparison, the ^{13}C CP-MAS spectra of the four samples are shown in Figure S2.

Monosaccharide analysis (Table 2) agrees well with the NMR spectra about the changes of the XyG concentrations with extraction (Tables S2 and S3), but reports lower absolute amounts of cellulose and XyG and higher amounts of pectins compared to the quantitative NMR spectra (Tables 2 and S4). One possible origin of this discrepancy is that sugar analysis reports the amount of RGI side chains (Ara and Gal) well, but Gal and Ara signals are not well resolved in the NMR spectra. Thus, the NMR-deduced total mass concentration of RGI is less accurate than the NMR-deduced backbone concentration of pectins. We estimated the total pectin molar amounts using a side chain/backbone mole ratio of 2.4–2.7, which was obtained from sugar analysis. Despite these uncertainties, the NMR and monosaccharide analyses agree on the trend of pectin reduction by sequential extraction.

Polysaccharide Hydration in the Intact Cell Wall. We first investigated the water content and water mobility of the four cell wall samples using ^{1}H NMR spectra (Figure 3). The spectra show similar integrated intensities of water within 20%, indicating that the total water content of the four cell walls is similar. However, the water ^{1}H line widths and T_1's differ significantly. The intact wall has the largest line width of 76 Hz and the shortest ^{1}H T_1 (0.12 s) (Table S5), whereas the extracted cell walls exhibit narrower water line widths of 9–27 Hz and longer T_1's of 0.9–1.4 s, which are closer to bulk water properties. Sample 2 has the narrowest water ^{1}H line width and the highest integrated intensity among the four samples,

dx.doi.org/10.1021/ja504108h | J. Am. Chem. Soc. 2014, 136, 10399–10409

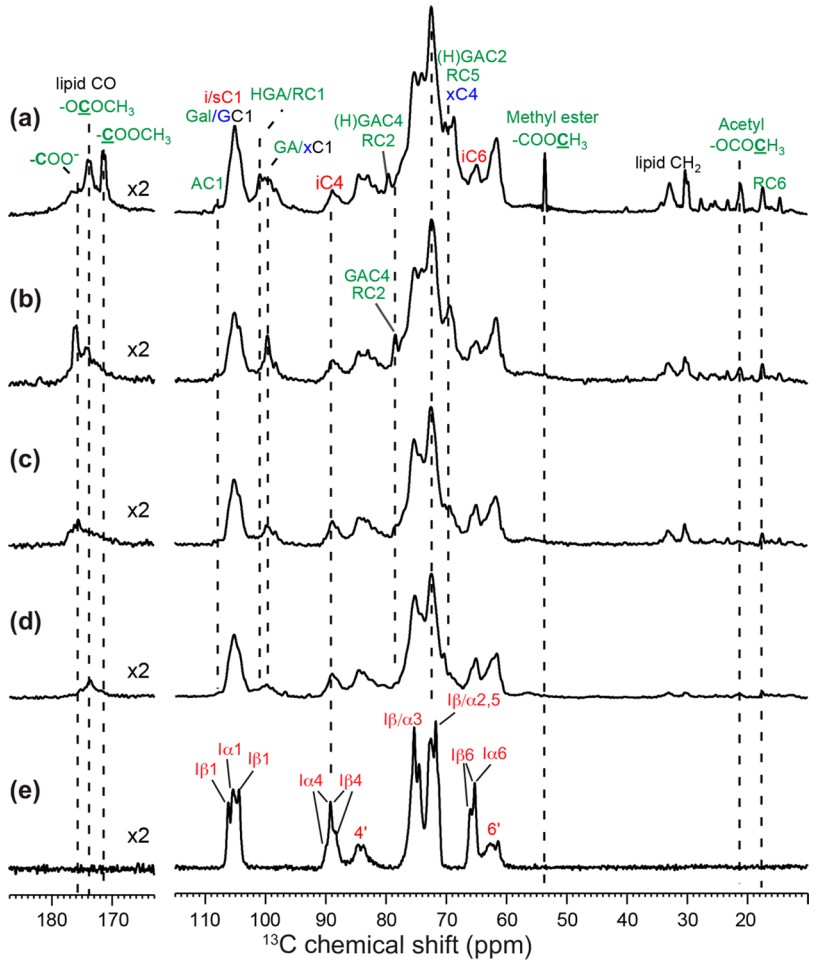

Figure 2. Quantitative 1D ^{13}C DP spectra of sequentially extracted *Arabidopsis* primary walls (a–d) and Avicel CP spectrum (e). (a) Intact cell wall (sample 1). (b) CDTA and Na_2CO_3 treated cell wall (sample 2). (c) Additional XEG treated cell wall (sample 3). (d) Additional Cel12A treated cell wall (sample 4). The matrix polysaccharide signals at 101, 80, 69, and 53 ppm (dashed lines) are preferentially suppressed by extraction, while the 89 ppm peak of crystalline cellulose C4 is little affected. The spectra are plotted with the same intensity for the 89 ppm of C4 peak. (e) ^{13}C CP-MAS spectrum of 40% hydrated Avicel. The signals of the two cellulose allomorphs, Iα and Iβ, can be resolved, and residual amorphous cellulose signals are annotated with a prime. All spectra were processed with Gaussian multiplication parameters of LB = −50 Hz and GB = 0.5.

indicating that it contains the most dynamic water. These line widths and T_1 differences indicate that water is more tightly bound to the intact wall than to the extracted walls, causing lower mobility and higher chemical exchange rates with the polysaccharides.[42]

Representative water–polysaccharide ^1H spin diffusion data are shown in Figure 4 for the intact wall sample. Water protons were selected as the magnetization source using a ^1H T_2 delay of 1.2–2.6 ms, which was optimized to preserve water magnetization maximally while suppressing most of the polysaccharide ^{13}C signals. The T_2 filter was unsynchronized with MAS so that recoupled anisotropic interactions better suppress the polysaccharide ^1H magnetization. Under these conditions, the polysaccharide ^{13}C signals were suppressed to <3% while 60–80% of the water intensity was retained. Some lipid ^1H signals also remained but accounted for less than 2% of the total ^1H magnetization; thus, they have negligible effects on water–polysaccharide spin diffusion. Due to the need to transfer the polysaccharide ^1H magnetization to ^{13}C by dipolar CP, the spin diffusion spectra preferentially enhance the signals of the rigid cellulose while reducing the signals of the dynamic pectins. However, at the experimental temperature of 263 K, the CP spectral deviation from the quantitative DP spectra is small, as shown in Figure S2. Thus, the majority of the matrix polysaccharides are captured in the spin diffusion data.

Turning on the spin diffusion mixing time for as little as 2 ms already caused significant polysaccharide ^{13}C signals (Figure 1c). The matrix polysaccharide intensities are enhanced relative to cellulose intensities. A series of 1D ^{13}C spectra with varying mixing times showed site-specific intensity buildup of the polysaccharides (Figure 4). Plotted as the square root of the mixing time to reflect the relayed nature of spin diffusion,[43,44] most ^{13}C signals exhibit a sigmoidal buildup: an initial slow transfer is followed by a fast linear regime that terminates in a plateau. All ^{13}C sites reached equilibrium by ~50 ms, and no intensity drop was observed, consistent with the fact that the water ^1H T_1 is much longer than 50 ms. The matrix polysaccharide peaks have the shortest equilibration times of 10–20 ms. In comparison, the crystalline cellulose peaks at 89 and 65 ppm display the slowest buildup, reaching equilibrium after ~35 ms. Since crystalline cellulose is not exposed to the microfibril surface, water polarization transfer is most likely relayed via surface cellulose through the ^1H–^1H dipolar coupling network of the microfibril. The buildup curves for the mixed matrix polysaccharide and cellulose peaks such as the 84 and 62 ppm peaks equilibrated at intermediate times of ~30

dx.doi.org/10.1021/ja504108h | J. Am. Chem. Soc. 2014, 136, 10399–10409

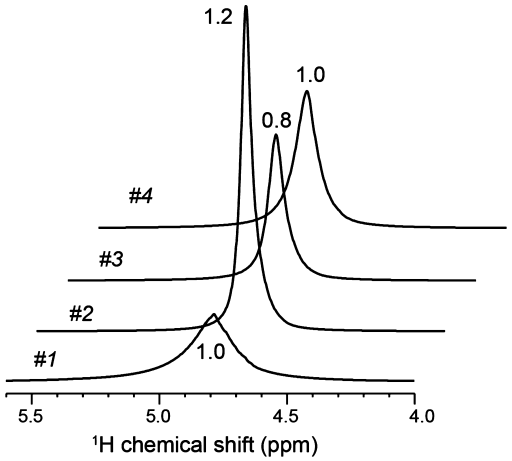

Figure 3. ^{1}H spectra of the four cell wall samples at 296 K. Numbers associated with each peak indicate the integrated intensities of the water peak as normalized to the value of the intact wall of sample 1. Sample 1 exhibits the largest water line width and the shortest ^{1}H T_1, indicating that water is well bound to the wall polysaccharides. The three extracted walls have narrower water line widths and longer T_1 values, indicating that water is less tightly bound to the polysaccharides.

ms, consistent with the mixed nature of these peaks. Pectin and XyG showed the largest intensity differences from cellulose in the initial regime of 2−6 ms: the former recovered 70−80% of the full magnetization while cellulose attained only 30−40% of the maximum intensity. XyG and pectin signals are not well resolved in these 1D ^{13}C spectra, thus only the average water contact of both matrix polysaccharides is reported from these 1D spin diffusion spectra. Taken together, these buildup curves indicate that water is much closer, and/or binds with much longer residence times, to pectins and hemicelluloses than to cellulose.

Hydration of Extracted Cell Walls. Partial extraction of pectins and hemicelluloses caused strikingly different water polarization transfer behaviors. For the CDTA/Na_2CO_3-treated sample 2, spin diffusion to both matrix polysaccharides and cellulose slowed down dramatically (Figure 5a). For example, the 69 ppm peak of GalA C2 and Rha C5 reached equilibrium at ∼150 ms instead of 15 ms in the intact wall, and the 89 ppm peak of crystalline cellulose equilibrated at 200 ms instead of 35 ms. Thus, the removal of calcium-cross-linked HG retarded water spin diffusion to the remaining polysaccharides. However, when half of the XyG is removed by XEG in sample 3, the spin diffusion rate partially recovered. The equilibration times shortened to ∼50 ms for the 69 ppm peak and ∼100 ms for cellulose, which are intermediate between the equilibration times of samples 1 and 2. Finally, further digestion by Cel12A in sample 4 fully restored the buildup rates, and cellulose intensities plateaued at about the same time as in the intact sample (Figure 5b). These buildup rate differences are not caused by centrifugal forces under 9 kHz spinning, since

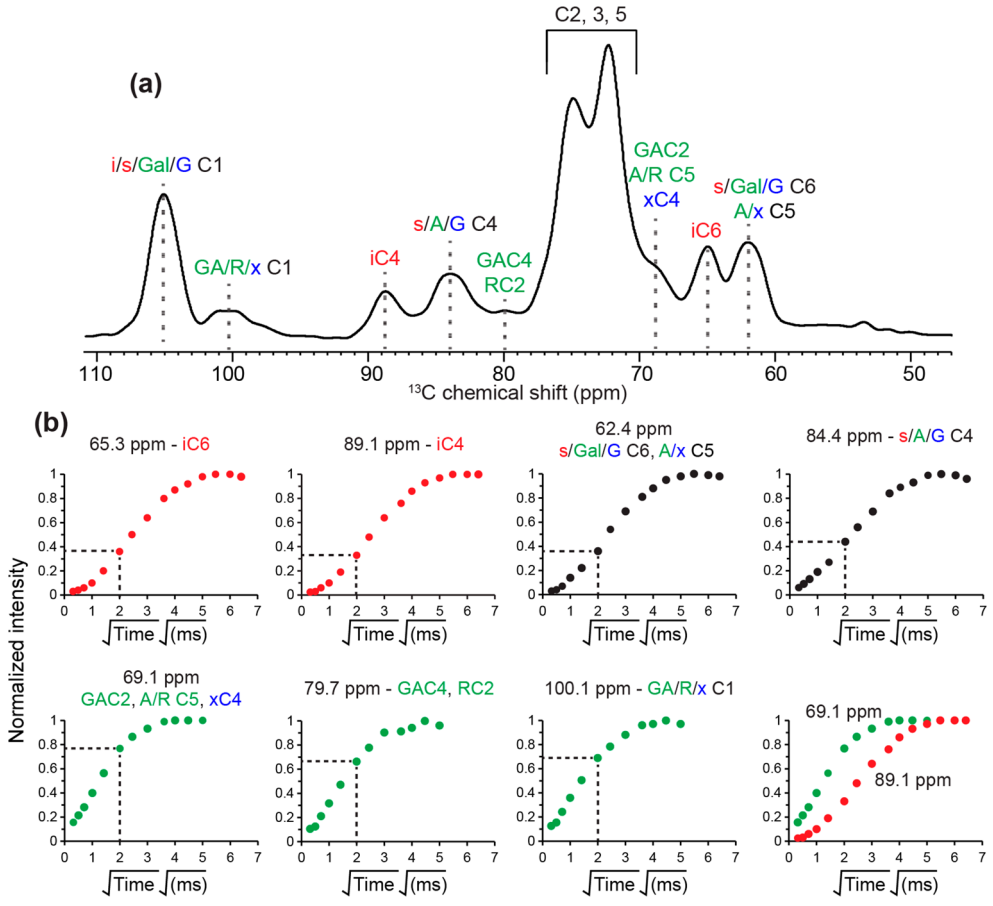

Figure 4. Water−polysaccharide spin diffusion buildup curves of sample 1. Mixing times ranged from 0.1 to 49 ms. (a) Assigned ^{13}C spectrum. (b) Buildup curves of the various peaks.

dx.doi.org/10.1021/ja504108h | J. Am. Chem. Soc. 2014, 136, 10399−10409

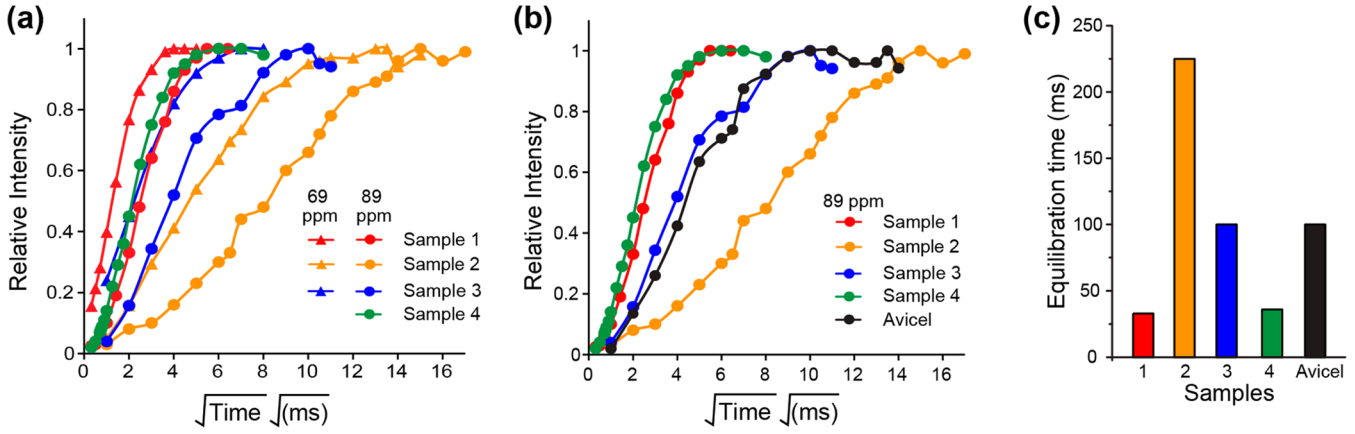

Figure 5. Comparisons of water−polysaccharide spin diffusion curves of different wall samples and Avicel. (a) Buildup curves of the 69 ppm peak of GalA C2 and Rha C5 and the 89 ppm peak of crystalline cellulose C4. (b) Buildup curves of crystalline cellulose C4 in samples 1−4 are shown separately for clarity, and are compared to the Avicel buildup curve. (c) Spin diffusion equilibration times of cellulose C4 in all five samples.

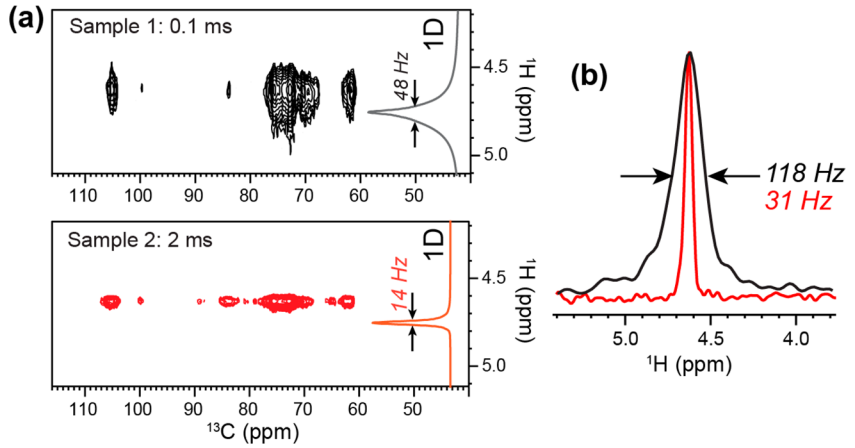

Figure 6. (a) 2D ^{1}H−^{13}C correlation spectra measured with mixing times of 0.1 ms for sample 1 (black) and 2 ms for sample 2 (red). The 1D ^{1}H spectrum, overlaid on the right of each 2D spectrum, shows a 0.1 ppm larger ^{1}H chemical shift for bulk water than for the polysaccharide-bound water seen in the 2D spectrum. (b) ^{1}H cross sections of the 2D spectra. Sample 2 (red) has a much narrower line width than sample 1, indicating that the polysaccharide-bound water in sample 2 is more dynamic than in sample 1.

slowing down the MAS frequency to 4.5 kHz reproduced the spin diffusion curves (Figure S3).

The fact that more extensive extractions in samples 3 and 4 caused more similar water−cellulose spin diffusion rates as sample 1 is interesting. This may be coincidental, but may also suggest that HG and RGI cause a similar hydration environment for cellulose compared to extracted walls with lower levels of both pectins. We then asked the question whether in the limit of no matrix polysaccharides, water−cellulose spin diffusion would be similar to that of the most extracted wall of sample 4. We chose commercial Avicel Ph-101, which is microcrystalline cellulose obtained from acid hydrolysis of wood pulp.[45,46] The ^{13}C CP-MAS spectrum (Figure 2e) of unlabeled and 40% hydrated Avicel shows well-resolved ^{13}C signals predominantly at crystalline cellulose chemical shifts, confirming that there are minimal amorphous cellulose and other polysaccharides.[47] Water spin diffusion to Avicel equilibrated at ∼100 ms (Figure 5b), similar to the buildup time of sample 3 but longer than the buildup time of sample 4.

Since water spin diffusion to polysaccharides depends on not only water proximity but also water mobility, we measured the ^{1}H line widths of water in close contact with polysaccharides using 2D ^{1}H−^{13}C correlation experiments. Figure 6 shows that the ^{1}H line widths of polysaccharide-proximal water follow the trend of the bulk water ^{1}H line widths: the intact wall has a broad ^{1}H line width of 118 Hz, whereas sample 2 has a much narrower line width of 31 Hz. Thus, the polysaccharide-proximal water is more dynamic in the extracted wall of sample 2 than in the intact wall. Interestingly, both samples show 0.1 ppm smaller ^{1}H chemical shifts for the polysaccharide-bound water in the 2D spectra than the bulk water in the 1D spectra. This ^{1}H chemical shift change may be caused by exchange between water and sugar moieties or weaker water−polysaccharide hydrogen-bonding compared to hydrogen-bonding in bulk water.

Water-Transferred 2D ^{13}C−^{13}C Correlation Spectra. Water−polysaccharide spin diffusion also provides a method to simplify the 2D correlation spectra. Figure 7 compares the full 2D spectrum with the water-transferred 2D spectrum measured with mixing times of 4 ms for sample 1 and 25 ms for sample 2. To allow comparison, we plotted the 2D spectra with equal multiplication factors from a minimum contour level of 1.3% of the maximum intensity, which is found at (72.2, 72.2) ppm. The full 2D spectrum of sample 1 showed prominent cellulose peaks such as C1−C2 (105, 72 ppm) and C4−C2/5 (89, 75 ppm), whereas matrix polysaccharide peaks such as Xyl C1−C2

dx.doi.org/10.1021/ja504108h | J. Am. Chem. Soc. 2014, 136, 10399−10409

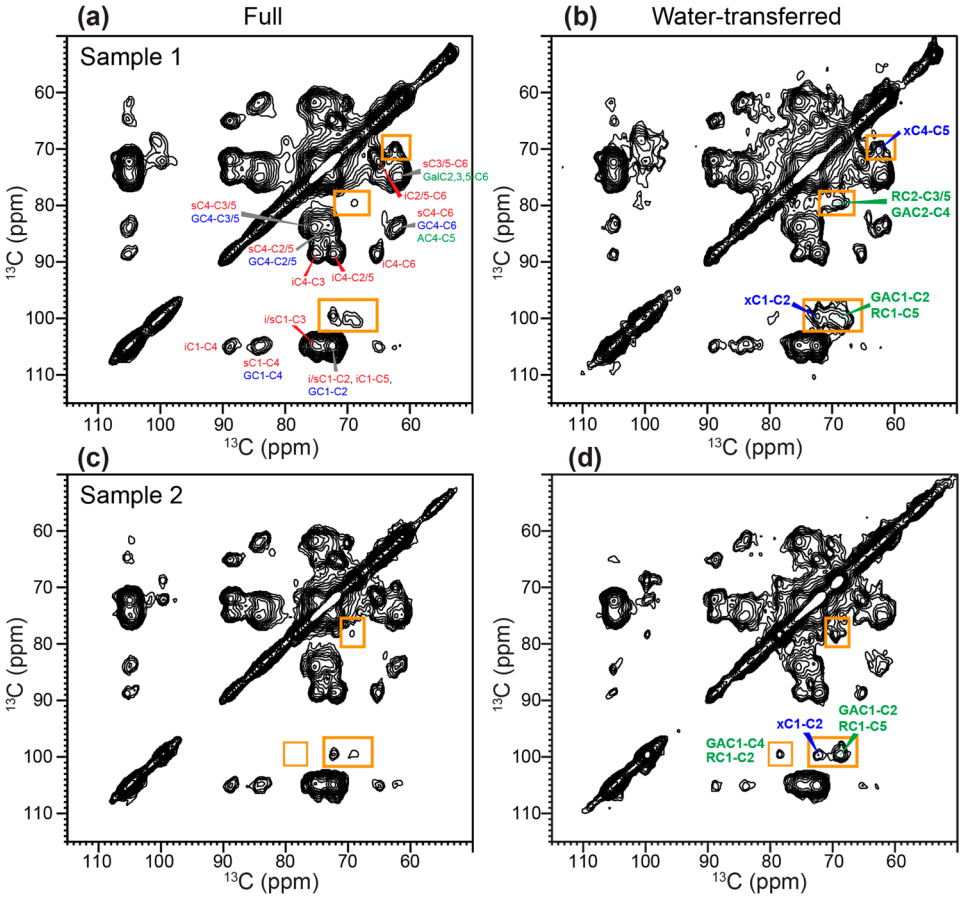

Figure 7. 2D ^{13}C DARR (10 ms) spectra without (a,c) and with (b,d) polarization transfer from water: (a,b) sample 1 and (c,d) sample 2. A ^{1}H T_2 filter of 1.7 ms was used, and the mixing times were 4 ms (b) and 25 ms (d). Fourteen contour levels were plotted from a minimum level of 1.3% of the highest peak of each spectrum with a multiplication factor of 1.3. Several well-resolved cross peaks of matrix polysaccharides are highlighted and assigned.

(99.5, 72.2 ppm) and C4−C5 (70.0, 62.3 ppm) are much weaker. In the water-transferred 2D spectrum, the matrix polysaccharide intensities increased relative to the cellulose peaks. The (79.4, 68.8 ppm) peak of Rha C2−C3/5 and GalA C2−C4 showed the largest intensity increase, and the XyG and pectin cross peaks at (99.5, 72.2 ppm) and (100.3, 68.7 ppm) are also enhanced. Interestingly, the water-transferred spectrum of sample 2 showed preferential enhancement of the pectin signals relative to XyG. For example, the RGI and HG cross peak at (100.3, 68.7 ppm) is ∼50% higher than the Xyl cross peak at (99.5, 72.2 ppm). This contrasts with the trend that this pectin peak is ∼20% weaker than the Xyl peak in the full 2D spectrum. Indeed, when the water-transferred 2D spectra were measured as a function of mixing time, the pectin peaks show slightly faster water transfer than the hemicellulose peaks (Figure S4). This difference was not observable from the 1D spin diffusion spectra (Figure 4) because of insufficient resolution. Thus, water interacts with pectins slightly more strongly than with hemicellulose.

DISCUSSION

These water−polysaccharide ^{1}H polarization transfer results can be summarized as follows. First, water polarization transfer to pectins is always faster than to cellulose in every sample, despite the fact that pectins are more mobile than cellulose. The latter is shown by the smaller C−H order parameters of pectins at ambient temperature (Figure S5) compared to cellulose. This pectin mobility partially remains at 263 K, which attenuates the ^{1}H−^{1}H dipolar couplings between water and pectins. Despite this pectin mobility, water−pectin polarization transfer is more rapid than water−cellulose transfer, indicating that water is either closer to pectins to give stronger ^{1}H−^{1}H dipolar couplings, and/or has a longer residence time on pectins than on cellulose. We attribute this time-averaged water−pectin proximity to the charged carboxylates and the polar methyl esters and acetyl groups in HG and RGI. In comparison, the lower hydration of cellulose can be attributed to the water-excluding assembly of glucan chains in the microfibril, and matrix polysaccharides may further reduce the water-exposed surface area of cellulose covering the cellulose microfibrils.

The second observation, which is more unexpected, is that the water−polysaccharide spin diffusion rates are significantly impacted by extraction: sample 2 exhibited the slowest spin diffusion while samples 1 and 4 showed the fastest spin diffusion. Since the total water content is similar for the four samples, and since sample 2 is the least extracted among the three extracted walls, this spin diffusion trend neither correlates with the extent of extraction nor correlates with the total water content.

We first considered the model where the slow spin diffusion of sample 2 may result from a smaller amount of polysaccharide-bound water after preferential extraction of HG. Although the total water content is similar among the four

dx.doi.org/10.1021/ja504108h | J. Am. Chem. Soc. 2014, 136, 10399−10409

samples, in principle the amount of polysaccharide-associated water could differ, with some water being separated into bulk. Among all polysaccharides, HG has the largest number of carboxyl and methyl ester groups, thus its preferential loss in sample 2 (Tables S1 and S2) might decrease the amount of water between cellulose microfibrils. However, close inspection of the quantitative ^{13}C spectra (Figure 2) shows that the carboxylate concentration is similar between samples 1 and 2, since the 176 ppm peak has similar integrated intensities. Thus, the model of wall dehydration due to reduced anion content does not agree with the NMR data.

Instead, the model that explains both the slow polarization transfer of sample 2 and the quantitative NMR spectra is that loss of Ca^{2+} by extraction significantly increased the water mobility in the wall so that spin diffusion is less efficient in sample 2. In the intact cell wall, Ca^{2+} ions tightly coordinate carboxylates and mediate HG gelation. Both the carboxylates and the HG network partly immobilize and entrap water molecules, whose magnetization can thus be efficiently transferred to the polysaccharides due to stronger $^{1}H-^{1}H$ dipolar couplings (Figure 8a). The bound nature of water in the intact wall is manifested by the larger water ^{1}H line width of sample 1 in both the 1D ^{1}H spectrum (Figure 3) and the 2D spectrum that detects polysaccharide-associated water (Figure 7).

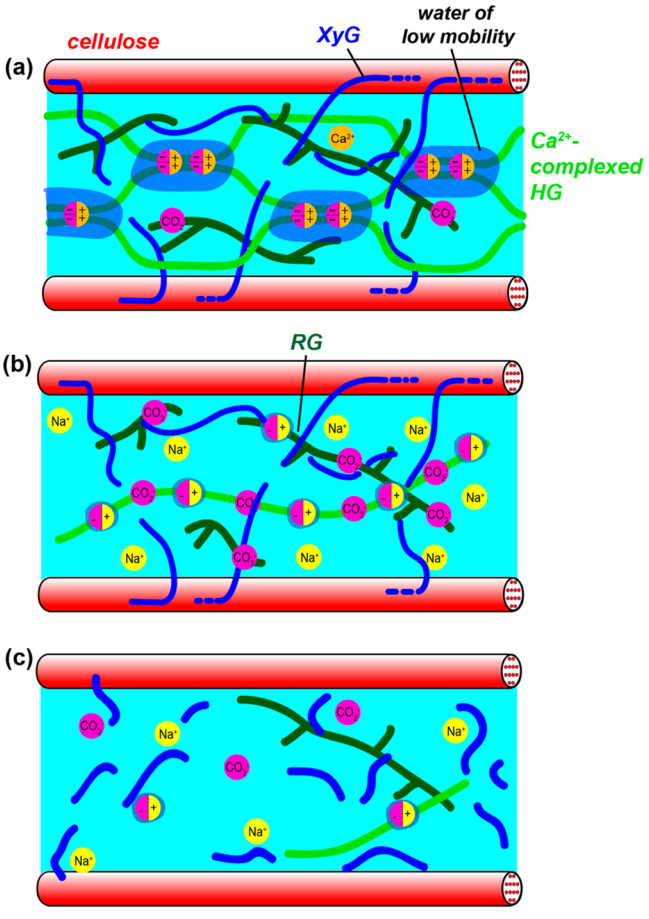

Figure 8. Model of water mobility and polysaccharide hydration in the *Arabidopsis* primary cell wall. (a) In the intact wall, Ca^{2+}-cross-linked HG chains create tightly bound water molecules that transfer polarization to polysaccharides efficiently. (b) Extraction of Ca^{2+} and solubilization of HG reduce the amount of bound water, thus slowing down spin diffusion. (c) When XyG is extracted together with other pectins, the remaining polysaccharides have larger water-exposed surface area, thus speeding up spin diffusion.

After Ca^{2+} ions were removed by CDTA, charge neutrality was maintained by sodium ions (Na^{+}) in solution, since the carboxylate concentrations remained constant between samples 1 and 2. These sodium ions are more weakly coordinated to the carboxylates and better solvated than Ca^{2+}.[48] The different bond strength between calcium carboxylate and sodium carboxylate is due to the higher absolute electronegativity of Ca^{2+} (31.6 eV) than Na^{+} (26.2 eV).[49] Indeed, electrical conductance of sodium-pectin samples is higher than that of calcium-pectin samples at the same hydration level.[48] In addition to ion solvation effects, monovalent ions such as Na^{+} and K^{+} do not cause HG gelation,[50] which further reduces the amount of bound water. The lower bound-water content of sample 2 is manifested by the narrower water ^{1}H line widths (Figures 3 and 6). Therefore, although the water content of sample 2 is slightly higher than sample 1, the larger water mobility slows down spin diffusion (Figure 8b).

It is worth noting that the effect of Ca^{2+} extraction on water mobility should not be confused with the effect of pectin de-esterification, and in fact the two effects are opposite of each other. Hydrolysis of methyl esters to carboxylates would promote the formation of calcium-chelated HG if Ca^{2+} ions were present, thus it should increase HG gelation, not decrease it, which would in turn increase the bound water content and speed up spin diffusion. The fact that the opposite was observed must thus be attributed uniquely to Ca^{2+} extraction and the consequent loss of HG and the loss of gelation.

The recovery of spin diffusion rates in samples 3 and 4 indicates a second factor regulating water–polysaccharide spin diffusion, which is the water-exposed surface area of the biopolymers. The increased digestions generate shorter XyG fragments and solubilize pectins, thus increasing the surface area of these matrix polysaccharides (Figure 8c). The digestion should also increase the water-exposed area of cellulose. It is difficult to estimate the relative increase of water exposure between matrix polysaccharides and cellulose, since water–cellulosic spin diffusion is likely relayed through matrix polysaccharides. This is suggested by the fact that spin diffusion rates changed uniformly and in the same direction for matrix polysaccharides and cellulose, and cellulose buildup lags behind matrix buildup in each sample.

The current results lend support to the single-network model of native plant walls concluded from 2D and 3D solid-state NMR spectra.[3−5] The fact that the water–cellulose spin diffusion rate changes in the same direction as water–pectin spin diffusion indicates a significant fraction of the microfibril surface to be loosely surrounded by pectins. Similarly, the fact that pectins are solubilized by XEG and Cel12A digestion supports the notion that pectins and XyG are intimately entangled, as seen by the intermolecular cross peaks in previous 2D and 3D spectra.[3−5]

Microcrystalline cellulose, which has a mixture of hydrophobic and hydrophilic surfaces with different hydration properties and bound-water structures,[15] showed comparable spin diffusion rates as cellulose in sample 3, despite the fact that sample 3 still contains matrix polysaccharides. This result suggests that the hydrophilicity of the cellulose surfaces in Avicel may be similar to the hydrophilicity of the cellulose microfibrils in the extracted cell wall.

dx.doi.org/10.1021/ja504108h | J. Am. Chem. Soc. 2014, 136, 10399−10409

The water mobility and accessibility information obtained here has no simple correlation with polysaccharide mobility.[3,4,11,51,52] High polysaccharide mobility does not necessarily lead to fast or slow polarization transfer from water. For example, water spin diffusion to mobile pectins is faster than spin diffusion to the rigid cellulose in each sample. On the other hand, spin diffusion to the rigid cellulose in sample 3 is faster than spin diffusion to mobile pectins in sample 2. Magnetic-resonance studies of water dynamics and water interactions in a wide range of biological and engineering materials such as cartilage[53] and cement[54] have unraveled rich information on the physicochemical properties of these materials. Most of these studies measure water relaxation times to infer water interactions with the matrix. The current study has the advantage of directly correlating water and matrix protons in a site-specific manner. This correlation and spin diffusion NMR approach can be readily extended into relaxation NMR studies of other hydrated chemical and biological systems.

CONCLUSIONS

These water−polysaccharide ^{1}H polarization transfer data provide molecular insights into the mobility of water and the amount of water-exposed surface areas of polysaccharides in non-grass primary cell walls. We found that calcium cross-links and HG gelation cause the formation of strongly bound water that transfers its polarization efficiently to surrounding polysaccharides. Calcium extraction and replacement by sodium ions reduce the number of tightly bound water molecules, thus slowing down spin diffusion to polysaccharides. Further extraction of matrix polysaccharides speeds up spin diffusion by increasing the water-exposed surface areas of polysaccharides. Thus, polysaccharide hydration is improved at later stages of extraction, after both pectins and hemicellulose are significantly depleted. The water−cellulose polarization transfer trend among the four cell wall samples follows the water−pectin polarization transfer trend, thus supporting the single-network model of the plant cell wall,[5] in which pectins have extensive molecular contact with cellulose. Comparative studies of the hydration of other cell walls such as grass cell walls and bacterial composites will be interesting in the future.

ASSOCIATED CONTENT

Supporting Information

Additional tables for polysaccharide composition analysis and NMR spectra. This material is available free of charge via the Internet at http://pubs.acs.org.

AUTHOR INFORMATION

Corresponding Author

meihong@mit.edu

Author Contributions

§P.B.W. and T.W. contributed equally to this work.

Notes

The authors declare no competing financial interest.

ACKNOWLEDGMENTS

Work at the Ames Laboratory is supported by DOE-BES under contract no. DE-AC02-07CH11358. Work at Penn State is supported by DOE-BES grant DE-FG02-84ER13179. Y.B.P. was supported by US-DOE-BES-EFRC Award DE-SC0001090.

REFERENCES

(1) Buchanan, B. B.; Gruissem, W.; Jones, R. L. *Biochemistry and Molecular Biology of Plants*; American Society of Plant Physiologists: Rockville, MD, 2000.

(2) Albersheim, P.; Darvill, A.; Roberts, K.; Sederoff, R.; Staehelin, A. *Plant Cell Walls*; Garland Science, Taylor&Francis Group, LLC: New York, 2010.

(3) Dick-Perez, M.; Wang, T.; Salazar, A.; Zabotina, O. A.; Hong, M. *Magn. Reson. Chem.* **2012**, *50*, 539−550.

(4) Dick-Perez, M.; Zhang, Y.; Hayes, J.; Salazar, A.; Zabotina, O. A.; Hong, M. *Biochemistry* **2011**, *50*, 989−1000.

(5) Wang, T.; Zabotina, O.; Hong, M. *Biochemistry* **2012**, *51*, 9846−9856.

(6) Bootten, T. J.; Harris, P. J.; Melton, L. D.; Newman, R. H. *J. Exp. Bot.* **2004**, *55*, 571−583.

(7) Park, Y. B.; Cosgrove, D. J. *Plant Physiol.* **2012**, *158*, 1933−1943.

(8) Cosgrove, D. J. *Plant Physiol.* **2001**, *125*, 131−134.

(9) Larsen, F. H.; Byg, I.; Damager, I.; Diaz, J.; Engelsen, S. B.; Ulvskov, P. *Biomacromolecules* **2011**, *12*, 1844−1850.

(10) Tang, H. R.; Belton, P. S.; Ng, A.; Ryden, P. *J. Agric. Food Chem.* **1999**, *47*, 510−517.

(11) Bootten, T. J.; Harris, P. J.; Melton, L. D.; Newman, R. H. *Biomacromolecules* **2009**, *10*, 2961−2967.

(12) Jarvis, M. C.; Fenwick, K. M.; Apperley, D. C. *Carbohydr. Res.* **1996**, *288*, 1−14.

(13) Hediger, S.; Emsley, L.; Fischer, M. *Carbohydr. Res.* **1999**, *322*, 102−112.

(14) Thakur, B. R.; Singh, R. K.; Handa, A. K. *Crit. Rev. Food Sci. Nutr.* **1997**, *37*, 47−73.

(15) Matthews, J. F.; Skopec, C. E.; Mason, P. E.; Zuccato, P.; Torget, R. W.; Sugiyama, J.; Himmel, M. E.; Brady, J. W. *Carbohydr. Res.* **2006**, *341*, 138−152.

(16) Hediger, S.; Lesage, A.; Emsley, L. *Macromolecules* **2002**, *35*, 5078−5084.

(17) Lesage, A.; Böckmann, A. *J. Am. Chem. Soc.* **2003**, *125*, 13336−13337.

(18) Huster, D.; Yao, X. L.; Hong, M. *J. Am. Chem. Soc.* **2002**, *124*, 874−883.

(19) Kumashiro, K. K.; Schmidt-Rohr, K.; Murphy, O. J.; Ouellette, K. L.; Cramer, W. A.; Thompson, L. K. *J. Am. Chem. Soc.* **1998**, *120*, 5043−5051.

(20) Li, S.; Su, Y.; Luo, W.; Hong, M. *J. Phys. Chem. B* **2010**, *114*, 4063−4069.

(21) Luo, W.; Hong, M. *J. Am. Chem. Soc.* **2010**, *132*, 2378−2384.

(22) Wang, T.; Park, Y. B.; Caporini, M. A.; Rosay, M.; Zhong, L.; Cosgrove, D. J.; Hong, M. *Proc. Natl. Acad. Sci. U.S.A.* **2013**, *110*, 16444−16449.

(23) Gibeaut, D. M.; Pauly, M.; Bacic, A.; Fincher, G. B. *Planta* **2005**, *221*, 729−738.

(24) Pauly, M.; Albersheim, P.; Darvill, A.; York, W. S. *Plant J.* **1999**, *20*, 629−639.

(25) Pauly, M.; Andersen, L. N.; Kauppinen, S.; Kofod, L. V.; York, W. S.; Albersheim, P.; Darvill, A. *Glycobiology* **1999**, *9*, 93−100.

(26) Nakazawa, H.; Okada, K.; Onodera, T.; Ogasawara, W.; Okada, H.; Morikawa, Y. *Appl. Microbiol. Biotechnol.* **2009**, *83*, 649−657.

(27) De Ruiter, G. A.; Schols, H.; Voragen, A. G. J.; Rombouts, F. M. *Anal. Biochem.* **1992**, *207*, 176−185.

(28) Morcombe, C. R.; Zilm, K. W. *J. Magn. Reson.* **2003**, *162*, 479−486.

(29) Liao, S. Y.; Fritzsching, K. J.; Hong, M. *Protein Sci.* **2013**, *22*, 1623−1638.

(30) Ader, C.; Schneider, R.; Seidel, K.; Etzkorn, M.; Becker, S.; Baldus, M. *J. Am. Chem. Soc.* **2009**, *131*, 170−176.

(31) Wang, T.; Yao, H.; Hong, M. *J. Biomol. NMR* **2013**, *56*, 139−148.

(32) Lesage, A.; Gardiennet, C.; Loquet, A.; Verel, R.; Pintacuda, G.; Emsley, L.; Meier, B. H.; Böckmann, A. *Angew. Chem., Int. Ed.* **2008**, *47*, 5851−5854.

(33) Lesage, A.; Emsley, L.; Penin, F.; Böckmann, A. *J. Am. Chem. Soc.* **2006**, *128*, 8246−8255.
(34) Bax, A.; Freeman, R.; Kempsell, S. P. *J. Am. Chem. Soc.* **1980**, *102*, 4849−4851.
(35) Lesage, A.; Auger, C.; Caldarelli, S.; Emsley, L. *J. Am. Chem. Soc.* **1997**, *119*, 7867−7868.
(36) Hong, M. *J. Magn. Reson.* **1999**, *136*, 86−91.
(37) Takegoshi, K.; Nakamura, S.; Terao, T. *Chem. Phys. Lett.* **2001**, *344*, 631−637.
(38) Hong, M.; Gross, J. D.; Rienstra, C. M.; Griffin, R. G.; Kumashiro, K. K.; Schmidt-Rohr, K. *J. Magn. Reson.* **1997**, *129*, 85−92.
(39) Bielecki, A.; Kolbert, A. C.; Levitt, M. H. *Chem. Phys. Lett.* **1989**, *155*, 341−346.
(40) Hong, M.; Griffin, R. G. *J. Am. Chem. Soc.* **1998**, *120*, 7113−7114.
(41) Rienstra, C. M.; Hohwy, M.; Hong, M.; Griffin, R. G. *J. Am. Chem. Soc.* **2000**, *122*, 10979−10990.
(42) Böckmann, A.; Gardiennet, C.; Verel, R.; Hunkeler, A.; Loquet, A.; Pintacuda, G.; Emsley, L.; Meier, B. H.; Lesage, A. *J. Biomol. NMR* **2009**, *45*, 319−327.
(43) Hong, M. *J. Phys. Chem. B* **2007**, *111*, 10340−10351.
(44) Hong, M.; Schmidt-Rohr, K. *Acc. Chem. Res.* **2013**, *46*, 2154−2163.
(45) Dourado, F.; Gama, F. M.; Chibowski, E.; Mota, M. *J. Adhesion Sci. Technol.* **1998**, *12*, 1081−1090.
(46) Park, S.; Baker, J. O.; Himmel, M. E.; Parilla, P. A.; Johnson, D. K. *Biotechnol. Biofuels* **2010**, *3*, 10.
(47) Yu, X. C.; Atalla, R. H. *Powder Technol.* **1998**, *98*, 135−138.
(48) Stuewer, R. F. *J. Phys. Chem.* **1938**, *42*, 305−315.
(49) Parr, R. G.; Pearson, R. G. *J. Am. Chem. Soc.* **1983**, *105*, 7512−7516.
(50) Thibault, J. F.; Rinaudo, M. *Biopolymers* **1985**, *24*, 2131−2143.
(51) Fenwick, K. M.; Apperley, D. C.; Cosgrove, D. J.; Jarvis, M. C. *Phytochemistry* **1999**, *51*, 17−22.
(52) Ha, M. A.; Apperley, D. C.; Jarvis, M. C. *Plant Physiol.* **1997**, *115*, 593−598.
(53) Lattanzio, P. J.; Marshall, K. W.; Damyanovich, A. Z.; Peemoeller, H. *Magn. Reson. Med.* **2000**, *44*, 840−851.
(54) Monteilhet, L.; Korb, J. P.; Mitchell, J.; McDonald, P. J. *Phys. Rev. E: Stat. Nonlin. Soft Matter Phys.* **2006**, *74*, 061404.

Supporting Information

Water – Polysaccharide Interactions in the Primary Cell Wall of *Arabidopsis thaliana* from Polarization Transfer Solid-State NMR

Paul B. White [1$], Tuo Wang [1$], Yong Bum Park [2], Daniel J. Cosgrove [2], and Mei Hong [1]*

[1] Department of Chemistry and Ames Laboratory, Iowa State University, Ames, IA 50011
[2] Department of Biology, Pennsylvania State University, University Park, PA 16802

Table S1. Relative intensities of polysaccharide peaks from 2D ^{13}C correlation spectra at 253 K.

Samples	Interior cellulose (89, 75) ppm [1]	Xyl in XyG (100, 72) ppm [2]	Pectin backbone (100, 69) ppm [3]	Rha (68, 17) ppm [4]	RG backbone (68, 17) ppm [5]	RG backbone 17 ppm [6]	Average RG backbone [7]	HGA [8]
1	1.0	1.1	1.3	0.19	1.0	1.0	1.0	1.0
2	1.0	0.94	0.95	0.18	0.99	0.79	0.9±0.1	0.64
3	1.0	0.75	0.74	0.10	0.56	0.51	0.54±0.03	0.59
4	1.0	0.43	0.52	0.08	0.44	0.32	0.38±0.06	0.39

[1.] The interior cellulose C4-C3 cross peak at (89, 75) ppm is used to normalize matrix polysaccharide intensities.

[2.] The (100, 72) ppm Xyl C1-C2 peak is used to quantify XyG amounts relative to cellulose. $I_{XyG} = I_{(100,72)} / I_{(89,75)}$

[3.] The (100, 69) ppm cross peak of GalA C1-C2 in RG I and HGA and Rha C1-C5 is used to represent the total pectin backbone concentration. $I_{Pectin} = I_{(100,69)} / I_{(89,75)}$.

[4.] The (68, 17) ppm cross peak of Rha C5-C6 represents the Rha amount. $I_{Rha} = I_{(68,17)} / I_{(89,75)}$.

[5.] The RG backbone concentration change from sample 1 is calculated by normalizing the Rha values with respect to that of sample 1.

[6.] The RG backbone concentration change was also estimated from the Rha C6 peak (17 ppm) intensity from the 1D quantitative ^{13}C spectra.

[7.] Consensus values of the RG concentration changes are calculated as the average of the 1D and 2D values.

[8.] The HGA concentration change is calculated as $I_{HGA} = \frac{\left(I_{100,69} - 2 \cdot I_{68,17}\right)_{sample\,i}}{\left(I_{100,69} - 2 \cdot I_{68,17}\right)_{sample\,1}}$. The factor of 2 accounts for the fact that the (100, 69) ppm cross peak contains one HGA peak and two RG peaks.

Table S2. Quantification of pectins based on 2D NMR spectral intensities of Rha and GalA.

Samples	Pectin backbone (100, 69) ppm	Rha (68, 17) ppm	RG sidechain[1]	RG amount [2]	HGA amount [3]	Pectin amount [4]	Pectin/Cellulose	
							NMR	Sugar
1	1.3	0.19	0.55	0.93	0.92	1.9	0.83 (100%)	2.7 (100%)
2	0.95	0.18	0.52	0.88	0.59	1.5	0.65 (78%)	1.7 (63%)
3	0.74	0.10	0.27	0.47	0.54	1.0	0.44 (53%)	2.1 (78%)
4	0.52	0.08	0.19	0.24	0.36	0.60	0.26 (31%)	1.7 (63%)

[1.] The RG sidechain quantity is calculated as the Rha amount times 2.4-2.7, which is the ratio obtained from sugar analysis.

[2.] The RG amount is calculated as $I_{RG} = I_{RG,sidchain} + 2I_{Rha}$.

[3.] The HGA amount is calculated as $I_{HGA} = I_{pectin} - 2I_{Rha}$.

[4.] The NMR-derived pectin amount is calculated as $I_{Pectin} = I_{RG} + I_{HGA}$.

Table S3. XyG quantification from 2D SSNMR data and from sugar composition analysis.

Samples	Interior cellulose	All cellulose [1]	Xyl in XyG [2]	XyG [3]	XyG : Cellulose ratio	
	(89, 75) ppm		(100, 72) ppm		NMR [4]	Sugar
1	1.0	2.3	1.1	2.5	1.1 (100%)	1.4 (100%)
2	1.0	2.3	0.94	2.2	0.94 (85%)	1.1 (84%)
3	1.0	2.3	0.75	1.7	0.75 (68%)	0.70 (51%)
4	1.0	2.3	0.43	0.86	0.43 (39%)	0.54 (39%)

[1.] The total amount of cellulose is estimated with a ratio of 1.0 : 1.3 between interior and surface cellulose. This ratio is obtained from a simulated cellulose model [1] and from 1D quantitative ^{13}C spectra.

[2.] The Xyl amount is estimated from the Xyl C1-C2 (100, 72) ppm peak intensity and normalized to the cellulose concentration.

[3.] The total amount of XyG is calculated as the sum of Glc and Xyl amounts, assuming a Glc : Xyl ratio of 4 : 3.

[4.] The NMR-derived XyG: cellulose molar ratio is calculated as the ratio of the XyG and all-cellulose concentrations. The relative value to sample 1 is given in brackets. The NMR quantification result overall agrees well with the sugar composition result.

Table S4. Amounts of the three classes of polysaccharides from all ^{13}C SSNMR data.

Samples	Cellulose[1]	XyG[2]	Pectins [3]
1	34%	37%	29%
2	39%	36%	25%
3	46%	34%	20%
4	57%	24%	19%

[1.] The cellulose amount includes both surface and crystalline cellulose.
[2.] The XyG amount includes both the Glc backbone and Xyl sidechains. The XyG: cellulose ratio is calculated in Table S3.
[3.] The pectin amount includes both HGA and RG-I, reported in Table S2.

Table S5. Water intensities and relaxation times in the four CW samples at 296 K [1].

Samples	Intensity [2]	^1H T_1 (s) [3]	^1H T_2 (ms)	Δ (Hz) [4]	Δ^* (Hz) [5]
1	1.0	0.12	5.7±0.4	56	76
2	1.2	1.2	194±17	1.6	9
3	0.8	0.88	33.3±0.5	9.6	17
4	1.0	1.38	25±1	13	27

[1.] Water intensities and relaxation times were measured on a Bruker DSX-400 MHz (9.4 T) spectrometer.
[2.] Water intensity is the integrated area of the water peak.
[3.] The ^1H T_1 was measured using a standard inversion recovery sequence.
[4.] The homogeneous linewidth is calculated from the measured ^1H T_2 of the water peak as $1/\pi T_2$.
[5.] The apparent linewidth is obtained from the full width at half maximum of the water peak.

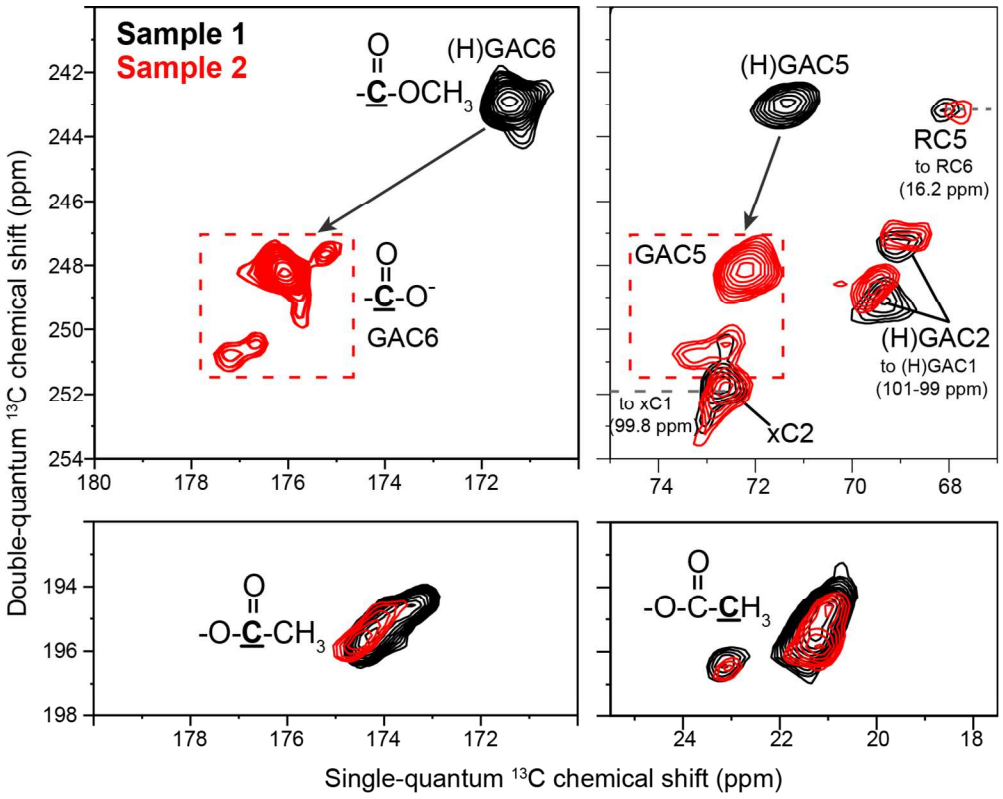

Figure S1. Pectin ^{13}C chemical shift changes between sample 1 and sample 2 due to extraction by chelating agents CDTA and sodium carbonate.

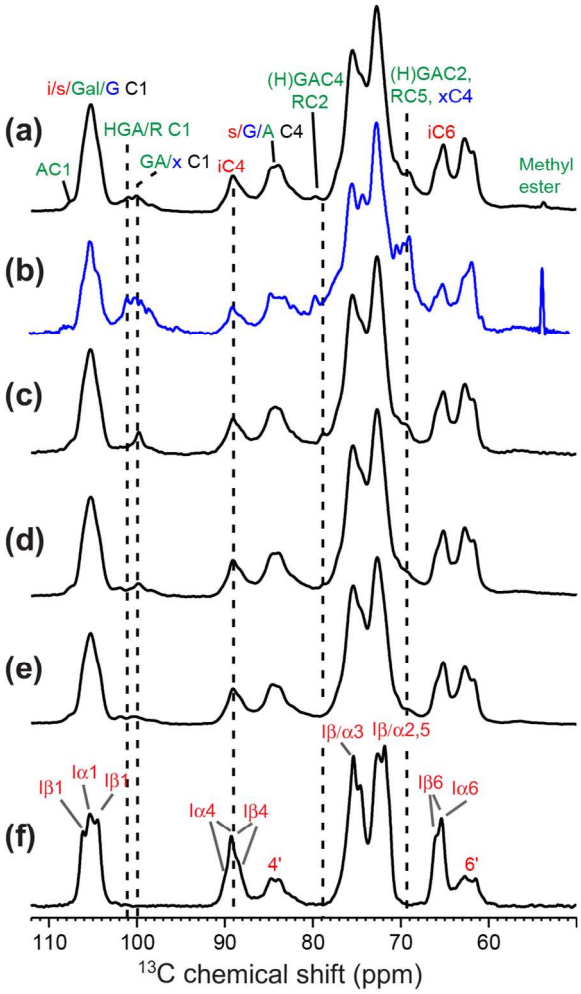

Figure S2. ^{13}C MAS spectra of sequentially digested Arabidopsis cell walls (a-e) and microcrystalline Avicel PH-101 (f). All spectra were measured at 296 K using CP except for (b), which was measured with DP in a quantitative manner. (a) CP spectrum of the intact cell wall (sample 1). (b) Quantitative ^{13}C DP spectrum of the intact cell wall. (c) CP spectrum of CDTA and sodium carbonate treated cell wall (sample 2). (d) CP spectrum of additional XEG-treated cell wall (sample 3). (e) CP spectrum of additional Cel12A treated sample (sample 4). (f) Avicel ^{13}C CP spectrum.

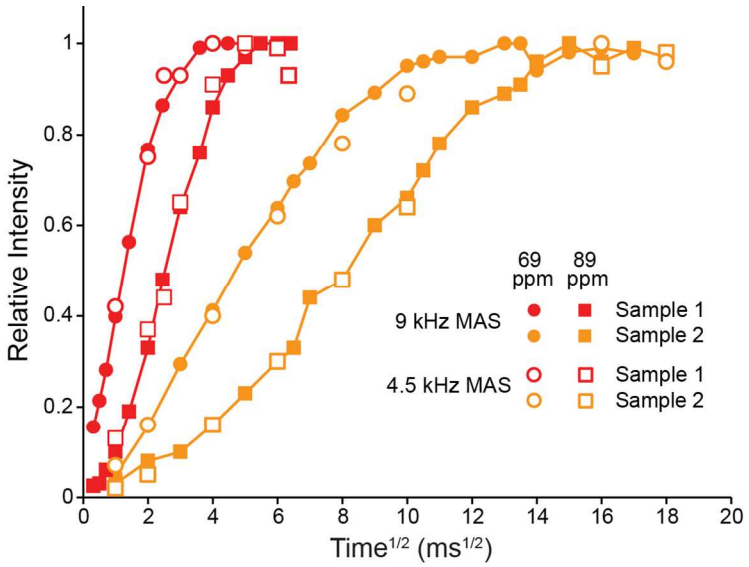

Figure S3. The water-to-polysaccharide spin diffusion is independent of the MAS frequency in the range used here (< 10 kHz). Buildup curves obtained from 9 kHz MAS (filled symbols) are indistinguishable from buildup curves obtained at the slower MAS frequency of 4.5 kHz. Thus, the centrifugal force due to MAS has negligible effects on water-to-polysaccharide spin diffusion.

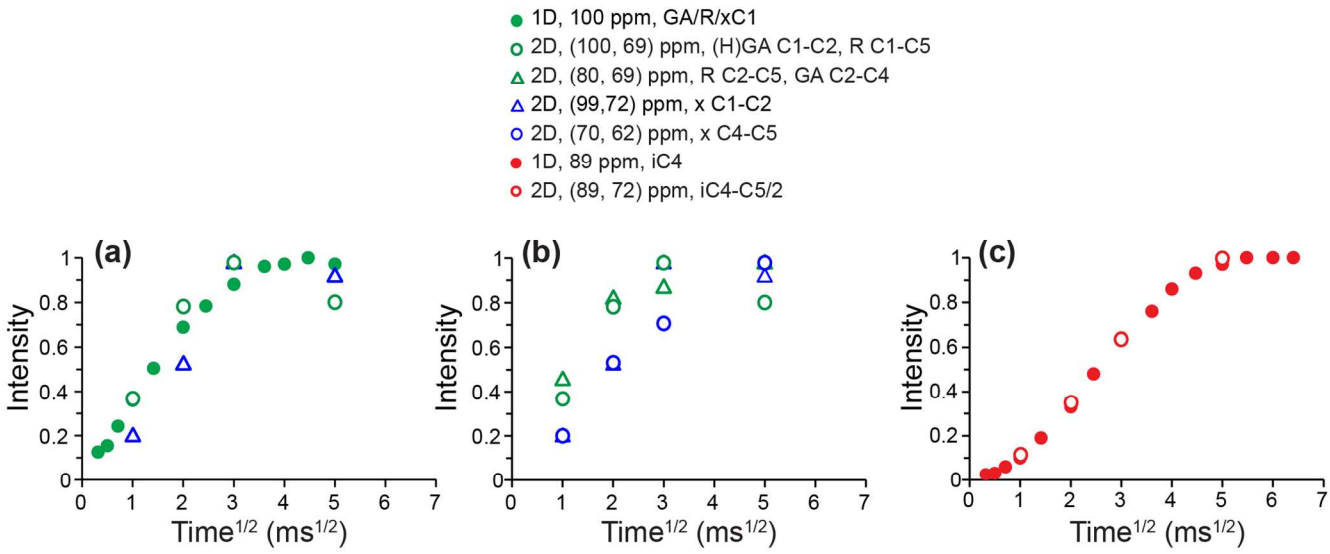

Figure S4. 2D water-edited ^{13}C correlation spectra resolve water spin diffusion to pectins and hemicellulose. The 1D buildup curves of the 100-ppm mixed peak of hemicellulose and pectins (filled green circles) and the 89-ppm peak of interior cellulose C4 (filled red circles) are compared with various 2D cross peaks. (a) Buildup curves of the (100, 69) ppm pectin cross peak and the (99, 72) ppm xylose cross peak straddle the buildup curve of the 100-ppm peak in the 1D spectra. The pectin buildup is faster than the hemicellulose buildup. (b) Buildup curves of several 2D cross peaks. Water spin diffusion to pectins is faster than to hemicellulose. (c) Buildup curve of the (89, 72) ppm cross peak of interior cellulose superimposes well with the buildup curve of the 1D 89-ppm peak.

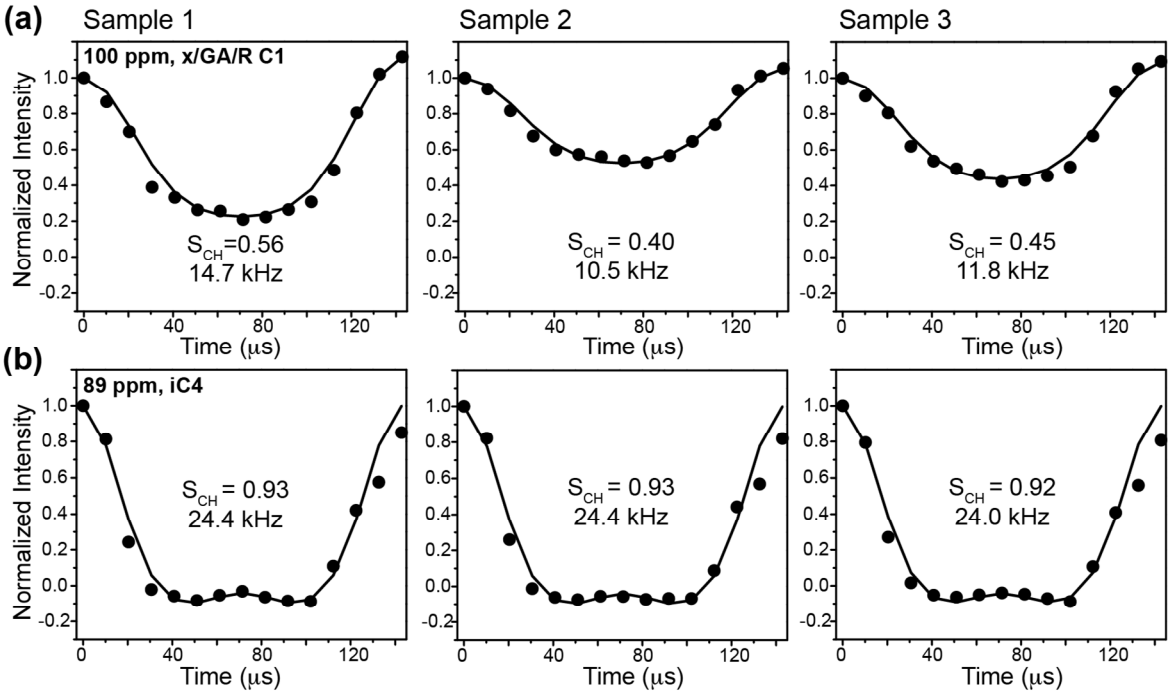

Figure S5. ^{13}C-^{1}H dipolar couplings of polysaccharides in three cell wall samples measured by the doubled DIPSHIFT experiment at 296 K under 7 kHz MAS. The C-H dipolar couplings (and order parameters) of matrix polysaccharides (a) decreased due to sequential extraction, indicating increased mobility, while the couplings of cellulose (b) are unaffected by digestion. The reported couplings are true values after taking into account the homonuclear decoupling scaling factor and the doubling factor.

References

(1) Wang, T.; Park, Y. B.; Caporini, M. A.; Rosay, M.; Zhong, L.; Cosgrove, D. J.; Hong, M. *Proc. Natl. Acad. Sci. U. S. A.* **2013**, *110*, 16444-16449.